Uniosun Journal of Engineering and Environmental Sciences (UJEES), Vol. 8 No. 3, March, 2026
DOI: 10.64980/ujees.v8i1.029 **Olaosebikan et al.**
Published: March 30, 2026

MATHEMATICAL ANALYSIS OF A TUBERCULOSIS CONTROL MODEL WITH VACCINATION, TREATMENT, AND PUBLIC AWARENESS VIA THE LAPLACE ADOMIAN METHOD

Mutiu Lawal OLAOSEBIKAN[1*], Joseph Adeleke ADEDEJI[2], Olatunji Abiodun FUNSHO[3], Ibrahim Adeshola ADEDIRAN[4], Timothy A OGUNLEYE[5]

[1,2,4,5] *Department of Mathematical Sciences, Osun State University P.M.B 4494, Osogbo, Osun State, Nigeria.*

[3] *Department of Computer Science, Federal Polytechnic Ede, Osun State, Nigeria*

[*]*Corresponding Author*: mutiu.olaosebikan@uniosun.edu.ng

Abstract
Tuberculosis remains a major public health challenge in many endemic regions. Populations with incomplete treatment coverage and limited awareness require an integrated control approach involving vaccination, timely treatment, and sustained public awareness. This study develops and analyses a mathematical model to evaluate the combined effects of vaccination, treatment, and awareness campaigns on tuberculosis transmission and control. The transmission model incorporating vaccination, treatment, and public awareness was formulated and shown to be well-posed using the Lipschitz condition, which guarantees existence and uniqueness of nonnegative solutions. The effective reproduction number was derived using the next-generation matrix method, while local stability of equilibrium points was examined using the Routh-Hurwitz criterion. Sensitivity analysis was conducted to identify parameters that influence transmission. The Laplace-Adomian decomposition method was used to obtain approximate analytical solutions, and simulations were carried out in Maple 18 to assess intervention scenarios. Results indicate that public awareness can substantially lower susceptibility and exposure over the simulated period, while childhood vaccination, adult vaccination, and improved treatment coverage reduce infection when combined. The findings support the use of integrated awareness, vaccination, and treatment strategies for tuberculosis control in settings with suboptimal treatment coverage. The study's main contribution is the combined-intervention threshold and associated sensitivity structure; the LADM implementation provides a semi-analytical solution framework rather than a direct efficiency comparison with Runge-Kutta methods.

Keywords
Tuberculosis; Basic reproduction number; Stability analysis; Laplace Adomian Decomposition Method

1. INTRODUCTION

Tuberculosis (TB) is an airborne infectious disease caused by Mycobacterium tuberculosis and is transmitted when people with active pulmonary TB expel infectious droplets that are inhaled by susceptible individuals [1]. Mathematical models are widely used to examine TB transmission, identify threshold conditions, and evaluate control strategies [2]-[5]. Previous studies have analysed incomplete treatment, exogenous reinfection, relapse, vaccination, and treatment-based control in TB models [5]-[10]. Semi-analytical approaches, including the Adomian decomposition method and the Laplace-Adomian decomposition method, provide useful approximate solutions for nonlinear epidemiological systems [11], [12]. The next-generation matrix and normalized sensitivity-index frameworks provide standard tools for deriving reproduction thresholds and ranking influential parameters [13], [14]. However, existing TB models often consider vaccination and treatment, or awareness-related reduction in transmission, as separate control mechanisms. Fewer studies integrate infant vaccination, adult vaccination, treatment efficacy, relapse, and public-awareness-mediated contact reduction in one deterministic threshold framework. This study addresses that gap by formulating a TB model with these combined interventions, deriving the effective reproduction threshold, assessing sensitivity structure, and applying LADM for approximate analytical simulation. The novelty lies in the combined-intervention threshold and sensitivity insight; the study does not claim a comparative efficiency assessment of LADM against RK4.

2. MATERIALS AND METHOD

2.1. Definition of Preliminaries

In this section, we introduce some fundamental concepts relevant to the present study. We also outline the Laplace Adomian decomposition method and discuss the qualitative behavior of the proposed mathematical model.

Definition 1: Let $\phi(t)$ be a sufficiently smooth function. The Laplace transform of its m th-order derivative is given by

$$\mathrm{L}\left[\frac{d^m\phi(t)}{dt^m}\right] = s^m\Phi(s) - s^{m-1}\phi(0) - s^{m-2}\phi'(0) - \cdots - \phi^{(m-1)}(0), \tag{1}$$

where $\Phi(s) = \mathrm{L}[\phi(t)]$.

Definition 2: Suppose an unknown function $U(t)$ can be expressed as an infinite series

$$U(t) = \sum_{k=0}^{\infty} U_k(t). \tag{2}$$

The Adomian polynomials $A_0, A_1, \ldots, A_n$ associated with a nonlinear operator $\mathrm{N}(U)$ are defined by

$$A_n = \frac{1}{n!}\frac{d^n}{d\lambda^n}\left[\mathrm{N}\left(\sum_{k=0}^{n} U_k\lambda^k\right)\right]\Bigg|_{\lambda=0}, \quad n \geq 0. \tag{3}$$

Definition 3: Let $\{x_n\}$ be a sequence and define the partial sums by

$$S_n = \sum_{k=1}^{n} x_k. \tag{4}$$

The infinite series $\sum_{k=1}^{\infty} x_k$ is said to be convergent if the sequence $\{S_n\}$ converges, that is,

$$\lim_{n\to\infty} S_n = S, \tag{5}$$

where S is a finite constant.

2.2. Laplace–Adomian Decomposition Method

Consider a general nonlinear ordinary differential equation of the form

$$\frac{d^m x(t)}{dt^m} = f(t, x(t)), \tag{6}$$

where $x(t)$ is the unknown function, $m \in \mathrm{N}$ denotes the order of the differential equation, and $f(t, x(t))$ is a given nonlinear function. To implement the Laplace–Adomian decomposition method, we first apply the Laplace transform to both sides of (6), yielding

$$\mathrm{L}\left[\frac{d^m x(t)}{dt^m}\right] = \mathrm{L}[f(t, x(t))]. \tag{7}$$

Using Definition 1, Eq. (7) becomes

$$s^m X(s) - s^{m-1}x(0) - s^{m-2}x'(0) - \cdots - x^{(m-1)}(0) = \mathrm{L}[f(t, x(t))], \tag{8}$$

where $X(s) = \mathrm{L}[x(t)]$. For simplicity, let

$$F(s) = \mathrm{L}[f(t, x(t))]. \tag{9}$$

Then Eq. (8) can be written as

$$s^m X(s) - \sum_{k=0}^{m-1} s^{m-1-k} x^{(k)}(0) = F(s). \tag{10}$$

For the particular case $m = 1$, Eq. (10) reduces to

$$sX(s) - x(0) = F(s), \tag{11}$$

which gives

$$X(s) = \frac{x(0)}{s} + \frac{1}{s}F(s). \tag{12}$$

Applying the inverse Laplace transform yields

$$x(t) = x_0(t) + \mathrm{L}^{-1}\left[\frac{1}{s}F(s)\right], \tag{13}$$

where $x_0(t) = x(0)$ represents the initial approximation.

The solution $x(t)$ is expressed as an infinite series

$$x(t) = \sum_{n=0}^{\infty} x_n(t). \tag{14}$$

Following Definition 2, the nonlinear term $f(t, x(t))$ is decomposed into a series of Adomian polynomials,

$$f(t, x(t)) = \sum_{n=0}^{\infty} A_n(t), \tag{15}$$

where the Adomian polynomials A_n are defined by

$$A_n = \frac{1}{n!}\frac{d^n}{d\lambda^n}\left[f\left(t, \sum_{k=0}^{n} x_k(t)\lambda^k \right)\right]\Bigg|_{\lambda=0}, \quad n \geq 0. \tag{16}$$

Substituting Eqs. (14) and (15) into Eq. (13) yields the recursive scheme

$$x_{n+1}(t) = \mathrm{L}^{-1}\left[\frac{1}{s}\mathrm{L}\left(A_n(t)\right)\right], \quad n \geq 0. \tag{17}$$

The approximate solution of order N is therefore given by

$$x(t) \approx \sum_{n=0}^{N} x_n(t). \tag{18}$$

According to Definition 3, the series solution (14) is convergent if

$$\lim_{n\to\infty} x_n(t) = 0, \tag{19}$$

in which case $\sum_{n=0}^{\infty} x_n(t)$ converges to the exact solution $x(t)$.

2.3. Model Description

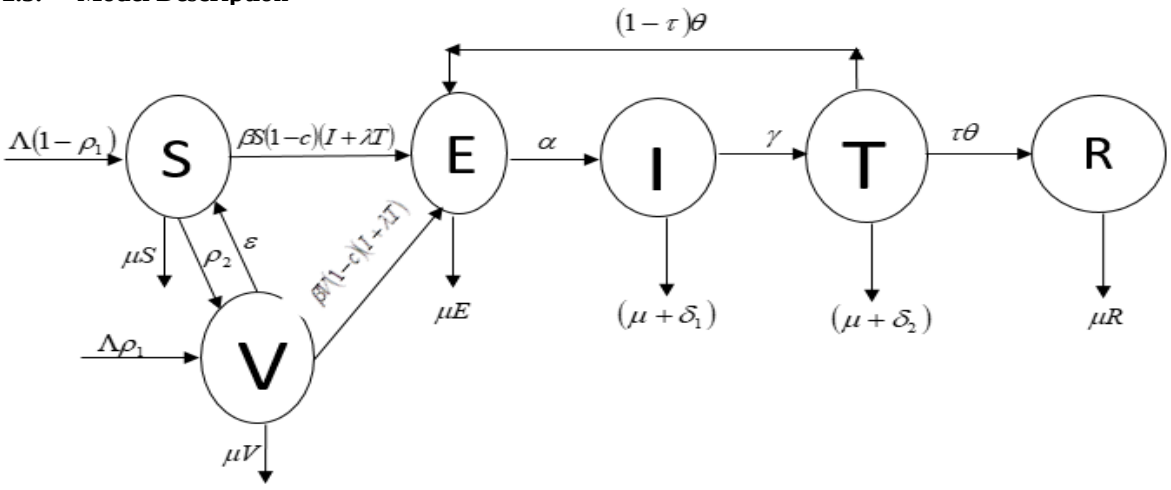

Figure 1: Schematic Flow of Model

Based on the flow diagram in Figure 1, the total population is classified into six compartments: susceptible, vaccinated, exposed, infectious (active TB), treated, and recovered individuals. Individuals are recruited into the population at the demographically scaled rate $\lambda = bN(0)$, where b is the annual per-capita birth rate and $N(0)$ is the initial total population. A proportion of recruits receives vaccination at birth. Vaccine protection diminishes at a waning rate, susceptible individuals may be vaccinated as adults, and susceptible or vaccinated individuals may acquire infection through contact with infectious or treated infectious

individuals. Public awareness reduces effective transmission by lowering risky contacts and promoting prevention-seeking behavior. Natural mortality and disease-induced mortality are included for the relevant compartments.

Exposed individuals develop active TB at rate α, while infectious individuals commence treatment at rate γ. Treated individuals leave the treatment class at rate θ, with a fraction $\tau\theta T$ recovering due to successful treatment and the remaining $(1-\tau)\theta T$ returning to the exposed class as a result of incomplete treatment, where $0 < \tau \leq 1$. Exposed individuals are assumed non-infectious, whereas treated individuals may still transmit TB. These assumptions govern the transmission dynamics and compartmental transitions described in equation (21).

$$\frac{dS(t)}{dt} = \Lambda(1-\rho_1) - \beta(1-c)S(t)\left[I(t)+\lambda T(t)\right] - (\mu+\rho_2)S(t) + \varepsilon V(t)$$

$$\frac{dV(t)}{dt} = \Lambda\rho_1 + \rho_2 S(t) - (\mu+\varepsilon)V(t) - m\beta(1-c)V(t)\left[I(t)+\lambda T(t)\right]$$

$$\frac{dE(t)}{dt} = \beta(1-c)\left[I(t)+\lambda T(t)\right]\left[S(t)+mV(t)\right] - (\mu+\alpha)E(t) + (1-\tau)\theta T(t) \quad (20)$$

$$\frac{dI(t)}{dt} = \alpha E(t) - (\mu+\delta_1+\gamma)I(t)$$

$$\frac{dT(t)}{dt} = \gamma I(t) - (\mu+\delta_2+\theta)T(t)$$

$$\frac{dR(t)}{dt} = \tau\theta T(t) - \mu R(t)$$

For simplicity, let: $g_1 = \Lambda(1-\rho_1)$, $g_2 = \beta(1-c_1), g_3 = (\mu+\rho_2)$, $g_4 = (\mu+\varepsilon)$, $g_5 = m\beta(1-c)$, $g_6 = (\mu+\alpha)$, $g_7 = (1-\tau)\theta$, $g_8 = (\mu+\delta_1+\gamma)$, $g_9 = (\mu+\delta_2+\theta)$, $g_{10} = \tau\theta$. Equation (20) simplifies to:

$$\frac{dS(t)}{dt} = g_1 - g_2 S(t)\left[I(t)+\lambda T(t)\right] - g_3 S(t) + \varepsilon V(t)$$

$$\frac{dV(t)}{dt} = \Lambda\rho_1 + \rho_2 S(t) - g_4 V(t) - g_5 V(t)\left[I(t)+\lambda T(t)\right]$$

$$\frac{dE(t)}{dt} = g_2\left[I(t)+\lambda T(t)\right]\left[S(t)+mV(t)\right] - g_6 E(t) + g_7\theta T(t) \quad (21)$$

$$\frac{dI(t)}{dt} = \alpha E(t) - g_8 I(t)$$

$$\frac{dT(t)}{dt} = \alpha E(t) - g_9 T(t)$$

$$\frac{dR(t)}{dt} = g_{10} T(t) - \mu R(t)$$

Subject to initial conditions:

$$S(0) = s_0 > 0, V(0) = v_0 > 0, E(0) = e_0 > 0, I(0) = i_0 > 0, T(0) = \eta_0 > 0, R(0) = r_0 > 0 \quad (22)$$

Table 1 lists the model parameters, descriptions, corrected numerical values, and sources. Because continuous daily TB outbreak data for direct fitting are limited, the simulation values are drawn from published literature, demographic scaling, and clearly stated modelling assumptions.

Table 1: Parameters, descriptions, corrected values, and sources used for simulations

Parameters	**Description**	**Values**	**References**
s_0	Initial population of susceptible individuals	4000	Assumed for simulation
v_0	Initial population of vaccinated individuals	2000	Assumed for simulation
e_0	Initial population of exposed individuals	600	Assumed for simulation
i_0	Initial population of infectious individuals	75	Assumed for simulation
η_0	Initial population undergoing treatment	50	Assumed for simulation
r_0	Initial population of recovered individuals	22	Assumed for simulation
δ_1	Disease-related mortality rate of infectious individuals	0.19 $year^{-1}$	[5]
δ_2	Disease-related mortality rate of treated individuals	0.08 $year^{-1}$	[5]
μ	Natural mortality rate	0.018 $year^{-1}$	[5]
Λ	Recruitment/birth rate, Lambda=bN(0)	b=0.03295 $year^{-1}$ $\Lambda = 222.34/year^{-1}$ N =6747	[15]
α	Progression rate from exposed/latent class to infectious class	0.365 $year^{-1}$ (0.001 day^{-1})	[10], [16]
τ	Treatment efficacy rate	0.5 (50%)	[5]
ρ_1	Infant vaccination rate	0.83 $year^{-1}$	[1], [17]
ρ_2	Vaccination rate of susceptible adults	0.3 $year^{-1}$ (30% coverage)	[8], [9]
λ	Relative infectiousness of treated individuals	0.07	[5]
β	Effective transmission rate of infectious individuals	0.0375 $year^{-1}$	[5], [8]
c	Public awareness effectiveness	0.3 (30%)	[9]
ε	Waning rate of vaccine-induced protection	0.05 $year^{-1}$	[6], [18]
θ	Treatment recovery rate	0.01 $year^{-1}$	[5]
γ	Treatment initiation rate	0.5 $year^{-1}$	[5]
m	Modification parameter for vaccinated infection risk	0.1 (dimensionless)	[8]

2.4. Analysis of Model Solution

We perform the qualitative analysis and semi-analytical approximation of the model solution in this section.

2.4.1. Existence, uniqueness and positivity of model solution

Establishing existence, uniqueness, and positivity of solutions to system (21) is essential to ensure that the model represents bounded and nonnegative human population dynamics for all t ≥ 0.

Theorem 1. The system of equations satisfies the local Lipschitz condition; that is, there exists a constant $L > 0$ such that for all t, t' in a neighborhood N of the initial conditions,

$$| D(X(t)) - D(X'(t)) | \leq L | X(t) - X'(t) |,$$

where $X(t) = (S, V, E, I, T, R)$.

Proof. From (22), define

$$\begin{aligned}
\zeta_1 &= g_1 - g_2 S(t)(I(t) + \lambda T(t)) - g_3 S(t) + \varepsilon V(t), \\
\zeta_2 &= \Lambda\rho_1 + \rho_2 S(t) - g_4 V(t) - g_5 V(t)(I(t) + \lambda T(t)), \\
\zeta_3 &= g_2(I(t) + \lambda T(t))(S(t) + mV(t)) - g_6 E(t) + g_7 \theta T(t), \\
\zeta_4 &= \alpha E(t) - g_8 I(t), \\
\zeta_5 &= \alpha E(t) - g_9 T(t), \\
\zeta_6 &= g_{10} T(t) - \mu R(t).
\end{aligned}$$

Each function ζ_i, $i = 1, \ldots, 6$, has bounded partial derivatives with respect to the state variables (S, V, E, I, T, R) in a neighborhood of the initial conditions. Hence, there exist constants $L_i > 0$ such that

$$\left| \frac{\partial \zeta_i}{\partial (S, V, E, I, T, R)} \right| \leq L_i.$$

Let $L = \max_{1 \leq i \leq 6} L_i$. Then the system satisfies the local Lipschitz condition, guaranteeing the existence and uniqueness of solutions. Moreover, since $L < \infty$, the solutions remain bounded and positive for all $t > 0$ in a neighborhood of R^6. This completes the proof.

Theorem 2. The solution of system (21) exists and is unique in R^6 for $\delta \geq 0$.

Proof. The result is established by showing that system (22) is positively invariant in R^4 for $\delta \geq 0$. For nonnegative initial conditions $S(0), V(0), E(0), I(0), T(0), R(0)$, all state variables remain nonnegative for all $t > 0$.

Evaluating the system on the boundary of the nonnegative orthant gives

$$\begin{aligned}
S'(t)\big|_{S=0} &= \Lambda(1-\rho_1) + \varepsilon V \geq 0, \qquad V'(t)\big|_{V=0} = \Lambda\rho_1 + \rho_2 S \geq 0, \\
E'(t)\big|_{E=0} &= \beta(1-c)(I + \lambda T)(S + mV) + (1-\tau)\theta T \geq 0, \\
I'(t)\big|_{I=0} &= \alpha E \geq 0, \qquad T'(t)\big|_{T=0} = \gamma I \geq 0, \qquad R'(t)\big|_{R=0} = \tau\theta T \geq 0.
\end{aligned} \tag{23}$$

Thus, the vector field points inward on the boundary of the positive orthant, ensuring that solutions remain in R_+^4. Consequently, the system admits a unique, nonnegative solution. With this result, we proceed to determine the equilibrium points of the model.

2.4.2. Disease free equilibrium

The disease-free equilibrium (DFE) corresponds to the absence of infection in the population. Hence, the exposed, infectious, and treated classes vanish, that is, $E = I = T = 0$. Setting the right-hand side of system (22) to zero and solving yields the DFE

$$\begin{aligned}
S_0 &= \frac{g_1(g_3 g_4 - \varepsilon\rho_2) + \varepsilon(g_1\rho_2 + \Lambda\rho_1 g_3)}{g_3(g_3 g_4 - \varepsilon\rho_2)}, \\
V_0 &= \frac{g_1\rho_2 + \Lambda\rho_1 g_3}{g_3 g_4 - \varepsilon\rho_2}, \\
E_0 &= I_0 = T_0 = R_0 = 0.
\end{aligned} \tag{24}$$

2.4.3. Endemic equilibrium

The endemic equilibrium represents a persistent presence of the disease in the population, where all compartments are nonzero. This equilibrium is important for understanding long-term disease dynamics and control strategies such as vaccination. Solving system (21) with $S, V, E, I, T, R \neq 0$ gives

$$S_* = \frac{g_1(g_9 g_4 + g_5 g_9 I^*(1+\lambda\gamma)) + g_9 \varepsilon \Lambda \rho_1}{(g_2 g_9 I^*(1+\lambda\gamma) - g_3 g_9)(g_4 g_9 + g_5 g_9 I^*(1+\lambda\gamma)) - \varepsilon \rho_2 g_9},$$

$$V_* = \frac{\Lambda \rho_1 g_2 g_9 (\gamma + g_9) + \rho_2 g_2 \gamma (g_6 + g_7)}{g_2(\rho_2 g_9 m + g_4 g_9 + g_5 I^*(g_9 + \lambda))(\gamma + g_9)}, \tag{25}$$

$$E_* = \frac{g_8}{\alpha} I^*, \qquad I_* = I^*, \qquad T_* = \frac{\gamma}{g_9} I^*, \qquad R_* = \left(\frac{g_{10}}{g_9} \frac{\gamma}{\mu} \right) I^*.$$

2.4.4. Linear stability analysis

This section investigates the local stability of the disease-free equilibrium (DFE). Linear stability analysis is carried out to assess the model's response to small perturbations introduced by the disease. Consider the Jacobian matrix of system (21) given by

$$J = \begin{pmatrix} -g_2(I+\lambda T) - g_3 & \varepsilon & 0 & -g_2 S & -g_2 \lambda S & 0 \\ \rho_2 & -g_4 & 0 & 0 & 0 & 0 \\ g_2(I+\lambda T) & g_2 m(I+\lambda T) & -g_6 & g_2(S+mV) & g_2\lambda(S+mV)+g_7 & 0 \\ 0 & 0 & \alpha & -\lambda & 0 & 0 \\ 0 & 0 & 0 & \gamma & -g_9 & 0 \\ 0 & 0 & 0 & 0 & g_{10} & -\mu \end{pmatrix}. \tag{26}$$

Evaluating the Jacobian at the disease-free equilibrium yields

$$J_0 = \begin{pmatrix} -g_3 & \varepsilon & 0 & -g_2 S_0 & -g_2 \lambda S_0 & 0 \\ \rho_2 & -g_4 & 0 & 0 & 0 & 0 \\ 0 & 0 & -g_6 & g_2(V_0 m + S_0) & g_2\lambda(V_0 m + S_0) + g_7 & 0 \\ 0 & 0 & \alpha & -\lambda & 0 & 0 \\ 0 & 0 & 0 & \gamma & -g_9 & 0 \\ 0 & 0 & 0 & 0 & g_{10} & -\mu \end{pmatrix}. \tag{27}$$

The eigenvalues are obtained from the characteristic equation

$$\det(J_0 - \lambda I) = 0. \tag{28}$$

Row reduction gives the eigenvalues

$$\lambda_1 = -\mu, \qquad \lambda_{2,3} = -\frac{1}{2}(g_3 + g_4 \pm \sqrt{(g_3 - g_4)^2 + 4\varepsilon\rho_2}), \tag{29}$$

which are all negative.

The remaining eigenvalues are obtained from the reduced subsystem

$$\begin{vmatrix} -g_6 - \lambda & g_2(V_0 m + S_0) & g_2\lambda(V_0 m + S_0) + g_7 \\ \alpha & -\lambda & 0 \\ 0 & \gamma & -g_9 - \lambda \end{vmatrix} = 0, \tag{30}$$

leading to the characteristic polynomial

$$\lambda^3 + (g_6 + g_9)\lambda^2 + (g_6 g_9 - \alpha g_2(V_0 m + S_0))\lambda - \alpha g_2(V_0 m + S_0)(g_9 + \lambda\gamma) - \alpha\gamma g_7 = 0. \tag{31}$$

Using

$$R_\varepsilon = \frac{g_2(V_0 m + S_0)\alpha(g_9 + \lambda\gamma)}{g_6 g_8 g_9 - \alpha\gamma g_7},$$

the polynomial can be rewritten as

$$\lambda^3 + \phi_1\lambda^2 + \phi_2\lambda + \phi_3 = 0, \tag{32}$$

where

$$\phi_1 = g_6 + g_9, \quad \phi_2 = g_6 g_9 - \alpha g_2(V_0 m + S_0), \quad \phi_3 = \alpha\gamma g_7(1 - R_\varepsilon) + R_\varepsilon g_6 g_8 g_9. \tag{33}$$

Since $\phi_1 > 0$, $\phi_3 > 0$ for $R_\varepsilon < 1$, and $\phi_1\phi_2 > \phi_3$, the Routh–Hurwitz conditions are satisfied. Hence, all eigenvalues have negative real parts, implying that the disease-free equilibrium is locally asymptotically stable.

2.4.5. Effective reproduction threshold R_0

The effective reproduction number R_e is a key epidemiological threshold that measures the average number of secondary infections generated by one infectious individual in the presence of control measures. Following the next-generation matrix framework [13], transmission persists when $R_e > 1$, whereas $R_e < 1$ indicates that the disease-free equilibrium is locally stable under the specified parameter regime. Mathematically, R_e is defined as the spectral radius $R_e = \rho(FV^{-1})$ of the next-generation matrix. Let the new infection and transition vectors be given by

$$f^* = \begin{pmatrix} g_2(I + \lambda T)(S + mV) \\ 0 \\ 0 \end{pmatrix}, \qquad V^* = \begin{pmatrix} g_6 E - g_7 T \\ -\alpha E + g_8 I \\ -\gamma I + g_9 T \end{pmatrix}.$$

From the Jacobian matrices of f^* and V^* with respect to the infected compartments (E, I, T), the matrices F and V are obtained as

$$F = \begin{pmatrix} 0 & g_2(S + mV) & g_2\lambda(S + mV) \\ 0 & 0 & 0 \\ 0 & 0 & 0 \end{pmatrix}, \qquad V = \begin{pmatrix} g_6 & 0 & -g_7 \\ -\alpha & g_8 & 0 \\ 0 & -\gamma & g_9 \end{pmatrix}.$$

The inverse of V is

$$V^{-1} = \frac{1}{\alpha\gamma g_7 - g_6 g_8 g_9} \begin{pmatrix} -g_8 g_9 & -g_7\gamma & -g_7 g_8 \\ -\alpha g_9 & -g_6 g_9 & -\alpha g_7 \\ -\alpha\gamma & -\gamma g_6 & -g_6 g_8 \end{pmatrix}. \tag{34}$$

Thus, the next-generation matrix $G = FV^{-1}$ becomes

$$G = \frac{-g_2(S + mV)\alpha(g_9 + \lambda\gamma)}{\alpha\gamma g_7 - g_6 g_8 g_9} \begin{pmatrix} 1 & * & * \\ 0 & 0 & 0 \\ 0 & 0 & 0 \end{pmatrix}. \tag{35}$$

The eigenvalues of G are

$$\lambda_1 = 0, \qquad \lambda_2 = 0, \qquad \lambda_3 = -\frac{g_2(S + mV)\alpha(g_9 + \lambda\gamma)}{\alpha\gamma g_7 - g_6 g_8 g_9}. \tag{36}$$

Hence, the spectral radius is

$$\sigma(G) = \frac{g_2(S + mV)\alpha(g_9 + \lambda\gamma)}{g_6 g_8 g_9 - \alpha\gamma g_7}. \tag{37}$$

Evaluating (37) at the disease-free equilibrium and substituting the expressions for g_2, g_6, g_7, g_8, and g_9 yields

$$R_\varepsilon = \frac{\Lambda\alpha\beta(1-c)(\lambda\gamma+\mu+\theta+\delta_2)(m\mu\rho_1+m\mu\rho_2-\mu\rho_1-\rho_1\rho_3+\varepsilon+\mu)}{((\mu+\varepsilon)(\mu+\rho_2)-\varepsilon\rho_2)(\alpha\gamma\theta(\tau-1)+(\mu+\alpha)(\mu+\delta_1+\gamma_1)(\mu+\delta_2+\theta))}. \quad (38)$$

Using parameter values from Table 1, the illustrative effective reproduction number is R_e= 0.2337322818 < 1, indicating local stability of the disease-free equilibrium for the chosen parameter set rather than a guaranteed field-level elimination outcome.

2.4.6. Quantitative analysis of the effective reproduction number

Here, the effective reproduction number is evaluated under standalone and combined intervention scenarios. The no-control threshold is R_e= 1.459137886 > 1, indicating that sustained transmission is expected in the absence of interventions. For each standalone scenario, one intervention parameter is varied while the remaining intervention parameters are held at their baseline values. For the combined scenario, vaccination, awareness, and treatment-related parameters are varied simultaneously. The resulting threshold values are presented in Tables 2 and 3.

Table 2: Standalone effects of vaccination and public awareness on the effective reproduction number.

Intervention level	**Infant vaccination only:** R_e	**Adult vaccination only:** R_e	**Public awareness only:** R_e
0.0	1.45913788	1.45913788	1.45913788
0.2	1.19649300	1.16731030	0.25434513
0.4	0.93384824	0.87548273	0.20246410
0.6	0.67120342	0.58365515	0.18416303
0.8	0.40855860	0.29182757	0.17481114
1.0	0.14591378	0.00000000	0.16913386

Table 3: Standalone treatment efficacy and combined-intervention effects on the effective reproduction number.

Intervention level	**Treatment efficacy only:** R_e	**Combined vaccination-awareness-treatment:** R_e
0.0	1.459137886	1.459137886
0.2	1.458149885	0.254345136
0.4	1.457163221	0.107760358
0.6	1.456177892	0.064354580
0.8	1.455193894	0.030256648
1.0	1.454211226	0.000000000

Tables 2 and 3 summarize the threshold response under standalone and combined interventions. In the standalone scenarios, infant vaccination, adult vaccination, and public awareness each reduce R_e, although their magnitudes differ. The treatment-only scenario produces only a modest reduction when untreated transmission persists. In contrast, simultaneous improvement of vaccination, awareness, and treatment parameters produces the largest decrease in R_e. These values should be interpreted as model-based threshold scenarios rather than direct predictions of complete disease elimination.

2.4.7. Sensitivity analysis of R_ε

In this section, the normalized sensitivity index is used to investigate the influence of model parameters on the effective reproduction number R_e.

Table 4 reports the sensitivity indices of the effective reproduction number R_e with respect to the model parameters, while Figure 2 illustrates these indices graphically. Parameters with positive sensitivity indices increase R_e and should be reduced where epidemiologically feasible. Parameters with negative sensitivity indices are mainly associated with vaccination, awareness, treatment, and treatment efficacy, and their increase suppresses transmission. Mortality-related parameters may also reduce R_e mathematically, but they are not actionable or desirable control strategies. The graphical summary is shown in Figure 2.

Table 4: Sensitivity indices of model parameters on the effective reproduction number

Parameters	Sensitivity indices
μ	-1.936256208
Λ	1
α	0.9060522180
τ	-0.01691063930
ρ_1	-0.1590226364
ρ_2	-0.4604145440
λ	0.01291512915
β	1
c	-0.4285714286
ε	0.4554685141
θ	-0.006804883923
γ	-0.5870171304
m	0.3724720297
δ_1	-0.2096049583
δ_2	-0.1614230096

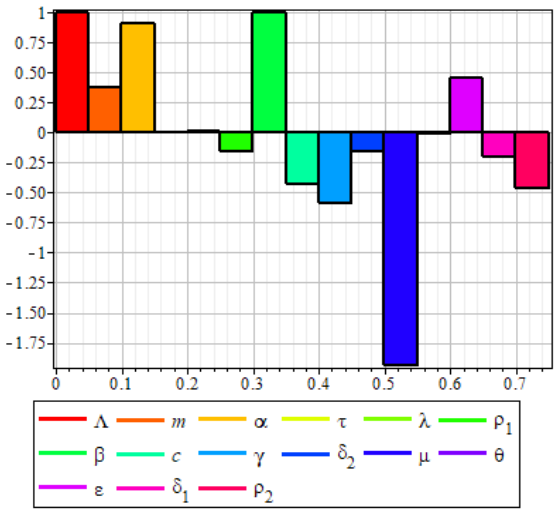

Figure 2: Sensitivity indices of the effective reproduction number with respect to model parameters

2.4.8. Numerical solution by LADM

In this section, we utilize the Laplace Adomian decomposition method to derive the solution of the model based on the demonstration outlined in the methodology. Thus, taking the Laplace transform of both sides,

$$L\left\{\frac{dS(t)}{dt}\right\} = L\left\{\Lambda(1-\rho_1) - \beta(1-c)S(t)\left[I(t)+\lambda T(t)\right] - (\mu+\rho_2)S(t) + \varepsilon V(t)\right\}$$

$$L\left\{\frac{dV(t)}{dt}\right\} = L\left\{\Lambda\rho_1 + \rho_2 S(t) - (\mu+\varepsilon)V(t) - m\beta(1-c)V(t)\left[I(t)+\lambda T(t)\right]\right\}$$

$$L\left\{\frac{dE(t)}{dt}\right\} = L\left\{\beta(1-c)\left[I(t)+\lambda T(t)\right]\left[S(t)+mV(t)\right] - (\mu+\alpha)E(t) + (1-\tau)\theta T(t)\right\} \quad (39)$$

$$L\left\{\frac{dI(t)}{dt}\right\} = L\left\{\alpha E(t) - (\mu + \delta_1 + \gamma) I(t)\right\}$$

$$L\left\{\frac{dT(t)}{dt}\right\} = L\left\{\gamma I(t) - (\mu + \delta_2 + \theta) T(t)\right\}$$

$$L\left\{\frac{dR(t)}{dt}\right\} = L\left\{\tau\theta T(t) - \mu R(t)\right\}$$

Applying Definition 1 to (39) we obtain

$$\begin{aligned}
vL\{S(t)\} - S(0) &= \frac{\Lambda(1-\rho_1)}{v} + L\{-\beta(1-c)S(t)[I(t)+\lambda T(t)] - (\mu+\rho_2)S(t) + \varepsilon V(t)\} \\
vL\{V(t)\} - V(0) &= \frac{\Lambda\rho_1}{v} + L\{+\rho_2 S(t) - (\mu+\varepsilon)V(t) - m\beta(1-c)V(t)[I(t)+\lambda T(t)]\} \\
vL\{E(t)\} - E(0) &= L\{\beta(1-c)[I(t)+\lambda T(t)][S(t)+mV(t)] - (\mu+\alpha)E(t) + (1-\tau)\theta T(t)\} \qquad (40) \\
vL\{I(t)\} - I(0) &= L\{\alpha E(t) - (\mu+\delta_1+\gamma)I(t)\} \\
vL\{T(t)\} - T(0) &= L\{\gamma I(t) - (\mu+\delta_2+\theta)T(t)\} \\
vL\{R(t)\} - R(0) &= L\{\tau\theta T(t) - \mu R(t)\}
\end{aligned}$$

Simplifying (40) yields

$$\begin{aligned}
L\{S(t)\} &= \frac{S(0)}{v} + \frac{\Lambda(1-\rho_1)}{v^2} + \frac{1}{v}\left(L\{-\beta(1-c)S(t)[I(t)+\lambda T(t)] - (\mu+\rho_2)S(t) + \varepsilon V(t)\}\right) \\
L\{V(t)\} &= \frac{V(0)}{v} + \frac{\Lambda\rho_1}{v^2} + \frac{1}{v}\left(L\{+\rho_2 S(t) - (\mu+\varepsilon)V(t) - m\beta(1-c)V(t)[I(t)+\lambda T(t)]\}\right) \\
L\{E(t)\} &= \frac{E(0)}{v} + \frac{1}{v}\left(L\{\beta(1-c)[I(t)+\lambda T(t)][S(t)+mV(t)] - (\mu+\alpha)E(t) + (1-\tau)\theta T(t)\}\right) \\
L\{I(t)\} &= \frac{I(0)}{v} + \frac{1}{v}\left(L\{\alpha E(t) - (\mu+\delta_1+\gamma)I(t)\}\right) \qquad (41) \\
L\{T(t)\} &= \frac{T(0)}{v} + \frac{1}{v}\left(L\{\gamma I(t) - (\mu+\delta_2+\theta)T(t)\}\right) \\
L\{R(t)\} &= \frac{R(0)}{v} + \frac{1}{v}\left(L\{\tau\theta T(t) - \mu R(t)\}\right)
\end{aligned}$$

Applying the initial conditions $S(0) = s_0$, $V(0) = v_0$, $E(0) = e_0$, $I(0) = i_0$, , $T(0) = \eta_0$, $R(0) = r_0$ and subsequently taking the inverse Laplace transform of (41) yields

$$\begin{aligned}
S(t) &= s_0 + \Lambda(1-\rho_1)t + L^{-1}\left[\frac{1}{v}\left(L\{-\beta(1-c)S(t)[I(t)+\lambda T(t)] - (\mu+\rho_2)S(t) + \varepsilon V(t)\}\right)\right] \\
V(t) &= v_0 + \Lambda\rho_1 t + L^{-1}\left[\frac{1}{v}\left(L\{+\rho_2 S(t) - (\mu+\varepsilon)V(t) - m\beta(1-c)V(t)[I(t)+\lambda T(t)]\}\right)\right] \\
E(t) &= e_0 + L^{-1}\left[\frac{1}{v}\left(L\{\beta(1-c)[I(t)+\lambda T(t)][S(t)+mV(t)] - (\mu+\alpha)E(t) + (1-\tau)\theta T(t)\}\right)\right] \qquad (42) \\
I(t) &= i_0 + L^{-1}\left[\frac{1}{v}\left(L\{\alpha E(t) - (\mu+\delta_1+\gamma)I(t)\}\right)\right] \\
T(t) &= \eta_0 + L^{-1}\left[\frac{1}{v}\left(L\{\gamma I(t) - (\mu+\delta_2+\theta)T(t)\}\right)\right]
\end{aligned}$$

$$R(t) = r_0 + L^{-1}\left[\frac{1}{v}\left(L\{\tau\theta T(t) - \mu R(t)\}\right)\right]$$

We can represent the unknown functions $S(t), V(t), E(t), I(t), T(t), R(t)$ as an infinite series:

$$S(t) = \sum_{u=0}^{\infty} S_u(t), V(t) = \sum_{u=0}^{\infty} V_u(t), E(t) = \sum_{u=0}^{\infty} E_u(t), I(t) = \sum_{u=0}^{\infty} I_u(t), T(t) = \sum_{u=0}^{\infty} T_u(t), R(t) = \sum_{u=0}^{\infty} R_u(t)\Bigg\}$$

The nonlinear terms are represented by:

$$\sum_{u=0}^{\infty} A_u(t) = S(t)I(t), \quad \sum_{u=0}^{\infty} B_u(t) = S(t)T(t), \quad \sum_{u=0}^{\infty} C_u(t) = V(t)I(t), \sum_{u=0}^{\infty} D_u(t) = V(t)T(t)$$

These nonlinear terms are decomposed using the Adomian Polynomial given by:

$$A_u(t) = \frac{1}{u!}\frac{d^u}{d\zeta^u}\left[\sum_{m=0}^{u}\zeta^m S_m(t)I_m(t)\right]_{\zeta=0}, B_u(t) = \frac{1}{u!}\frac{d^u}{d\zeta^u}\left[\sum_{m=0}^{u}\zeta^m S_m(t)T_m(t)\right]_{\zeta=0}\Bigg\}$$

$$C_u(t) = \frac{1}{u!}\frac{d^u}{d\zeta^u}\left[\sum_{m=0}^{u}\zeta^m V_m(t)I_m(t)\right]_{\zeta=0}, D_u(t) = \frac{1}{u!}\frac{d^u}{d\zeta^u}\left[\sum_{m=0}^{u}\zeta^m V_m(t)T_m(t)\right]_{\zeta=0}\Bigg\},$$

$$\sum_{u=0}^{\infty} V_{u+1}(t) = v_0 + \Lambda\rho_1 t + L^{-1}\left[\frac{1}{v}\left(L\left\{+\rho_2\sum_{u=0}^{\infty}S_u(t) - (\mu+\varepsilon)\sum_{u=0}^{\infty}V(t) - m\beta(1-c)\left[\sum_{u=0}^{\infty}C(t) + \lambda\sum_{u=0}^{\infty}D(t)\right]\right\}\right)\right]$$

$$\sum_{u=0}^{\infty} E_{u+1}(t) = e_0 + L^{-1}\left[\frac{1}{v}\left(L\left\{\beta(1-c)\left(\begin{array}{l}\sum_{u=0}^{\infty}A_u(t) + m\sum_{u=0}^{\infty}C_u(t)\\ +\lambda\sum_{u=0}^{\infty}B_u(t) + m\lambda\sum_{u=0}^{\infty}D_u(t)\end{array}\right) - (\mu+\alpha)\lambda\sum_{u=0}^{\infty}E_u(t) + (1-\tau)\theta\lambda\sum_{u=0}^{\infty}T_u(t)\right\}\right)\right]$$

$$\sum_{u=0}^{\infty} I_{u+1}(t) = i_0 + L^{-1}\left[\frac{1}{v}\left(L\left\{\alpha\sum_{u=0}^{\infty}E_u(t) - (\mu+\delta_1+\gamma)\sum_{u=0}^{\infty}I_u(t)\right\}\right)\right]$$

$$\sum_{u=0}^{\infty} T_{u+1}(t) = \eta_0 + L^{-1}\left[\frac{1}{v}\left(L\left\{\gamma\sum_{u=0}^{\infty}I_u(t) - (\mu+\delta_2+\theta)\sum_{u=0}^{\infty}T_u(t)\right\}\right)\right]$$

$$\sum_{u=0}^{\infty} R_{u+1}(t) = r_0 + L^{-1}\left[\frac{1}{v}\left(L\left\{\tau\theta\sum_{u=0}^{\infty}T_u(t) - \mu\sum_{u=0}^{\infty}R_u(t)\right\}\right)\right] \tag{43}$$

Comparing the linear terms of recurrence relation in equation (43), the initial approximation results for the model variables are obtained as:

$$S_0(t) = s_0 + \Lambda(1-\rho_1)t,\ V_0(t) = v_0 + \Lambda\rho_1,\ E_0(t) = e_0,\ I_0(t) = i_0, T_0(t) = \eta_0,\ R_0(t) = r_0 \tag{44}$$

The first approximate results are obtained by evaluating system (48) at u=0 so that

$$S_1(t) = \begin{pmatrix}\beta c\lambda\eta_0 s_0 + \beta c i_0 s_0\\ -\beta\lambda\eta_0 s_0 - \beta i_0 s_0 + \varepsilon v_0\end{pmatrix}t + \begin{pmatrix}-\Lambda\beta c\lambda\eta_0\rho_1 + \Lambda\beta c\lambda\eta_0\\ -\Lambda\beta c i_0\rho_1 + \Lambda\beta\lambda\eta_0\rho_1\\ +\Lambda\beta c i_0 - \Lambda\beta\lambda\eta_0 + \Lambda\beta i_0\rho_1\\ -\Lambda\beta i_0 + \Lambda\varepsilon\rho_1 - \mu s_0 - s_0\rho_2\end{pmatrix}\frac{t^2}{2} + \left(\Lambda\mu\rho_1 + \Lambda\rho_1\rho_2 - \Lambda\mu - \Lambda\rho_2\right)\frac{t^3}{6}$$

$$V_1(t) = \begin{pmatrix}\rho_2 s_0 - \mu v_0 - \varepsilon v_0 - \beta m i_0 v_0 - \beta m\eta_0 v_0\lambda\\ +\beta c m i_0 v_0 + \beta c\lambda m\eta_0 v_0\end{pmatrix}t + \begin{pmatrix}\Lambda\rho_2 - \Lambda\rho_1\rho_2 - \Lambda\rho_1\mu - \Lambda\varepsilon\rho_1 - \Lambda\beta\lambda m_0\eta_0\rho_1\\ +\Lambda\beta c m i_0\rho_1 + \Lambda\beta c\lambda m\eta_0\rho_1 - \Lambda\beta m i_0\rho_1\end{pmatrix}\frac{t^2}{2}$$

$$E_1(t) = \begin{pmatrix}\theta\eta_0 - \mu e_0 - \alpha e_0 + \tau\theta\eta_0 + \beta s_0 i_0\\ -\beta c i_0 s_0 + \beta\lambda m\eta_0 v_0 - \beta c\lambda m\eta_0 v_0\end{pmatrix}t + \begin{pmatrix}\Lambda\beta i_0 - \Lambda\beta i_0\rho_1 - \Lambda\beta c i_0 + \Lambda\beta c i_0\rho_1\\ +\Lambda\beta\lambda m\eta_0\rho_1 - \Lambda\beta c\lambda m\eta_0\rho_1\end{pmatrix}\frac{t^2}{2} \tag{45}$$

$$I_1(t) = (\alpha e_0 - (\mu + \delta_1 + \gamma) i_0)t$$
$$T_1(t) = (\gamma i_0 - (\mu + \delta_2 + \theta)\eta_0)t$$
$$R_1(t) = (\tau\theta\eta_0 - \mu r_0)t$$

Higher-order approximate results can be computed by implementing the recurrence relation in Maple 18 software. Two more iterations are performed to obtain the power series solution of the system given by

$$\left.\begin{aligned} S(t) = \sum_{u=0}^{3} S_u(t), V(t) = \sum_{u=0}^{3} V(t),\ E(t) = \sum_{u=0}^{3} E_u(t), \\ I(t) = \sum_{u=0}^{3} I_u(t), T(t) = \sum_{u=0}^{3} T_u(t), R(t) = \sum_{u=0}^{3} R_u(t) \end{aligned}\right\}$$

3. RESULTS AND DISCUSSION

In this section, we conduct a numerical evaluation of the model results and discuss convergence of the obtained solution. Using the baseline parameter values in Table 1 and the series solution in equation (51), the model solutions are evaluated as follows:

$$\begin{aligned} S(t) &= 4000 - 8141.578600t + 10398.92455t^2 - 11166.74565t^3 - 933.7405786t^4 \\ &\quad - 20.80064391t^5 - 0.1794208089t^6 - 0.587894004 \cdot 10^{-5} t^7 \\ V(t) &= 2000 + 656.3736000t - 1179.673235t^2 + 1133.087908t^3 + 69.45672550t^4 \\ &\quad + 1.014279416t^5 + 0.388231890 \cdot 10^{-4} t^6 \\ E(t) &= 600 + 7881.185000t - 10812.84778t^2 + 11498.95864t^3 + 647.1288413t^4 \\ &\quad + 6.668313583t^5 + 0.254777178 \cdot 10^{-3} t^6 \\ I(t) &= 75 - 51.9600t + 25.88096575t^2 - 12.95604483t^3 - 0.1988171047t^4 - 0.913352148 \cdot 10^{-5} t^5 \end{aligned} \quad (52)$$

$$T(t) = 50 + 26.600t - 15.88940000t^2 + 5.468124025t^3 + 0.734404281 \cdot 10^{-4} t^4$$
$$R(t) = 22 - 0.146t + 0.067814\, t^2 - 0.02688921733t^3$$

3.1. Convergence Analysis

In this section, we examine the convergence of the obtained series solution in (52).

Theorem 3: The LADM series is a generalized solution of (13) on [a,b] if the corresponding positive-term comparison series converges. Proof: By D'Alembert's ratio test, convergence follows when the ratio of successive terms is less than one. Therefore, the LADM series converges under the stated ratio-test condition.

Lemma 1: From Theorem 3, the solution of the mathematical model (14) given by (52) converges.

Proof: Following the convergence criterion for the Adomian decomposition method [19], the power-series solution converges when the ratio condition in (53) is less than one.

Following the proof of Theorem 1 and Lemma 1, Table 5 gives the numerical implication of the ratio test.

The ratio-test results in Table 5 are all less than one. Hence, the solution series is convergent under the stated criterion.

3.2. Simulation results

The simulations show how the model responds to public awareness, childhood vaccination, adult vaccination, and treatment. Public awareness reduces the susceptible and exposed compartments in the simulated scenario, but this should be interpreted as a model-based decline toward a very low level rather than as literal eradication of all susceptible individuals within six months. In Figure 3, higher awareness lowers effective transmission, decreases susceptibility, and reduces exposure over the simulated period. Figures 4 and 5 indicate that childhood and adult vaccination increase vaccine-protected individuals and reduce exposure; these trajectories are scenario comparisons under assumed parameter values, not guaranteed field outcomes. Figure 6A shows that high treatment efficacy reduces the infectious compartment. Figure 6B should be interpreted as the transient behavior of the recovered compartment under the model's treatment and outflow assumptions. Successful treatment is inferred from reduced active infection and reduced relapse potential, not from the recovered class declining to zero. Overall, the simulations support public awareness, vaccination, and efficient treatment as complementary controls for lowering TB transmission.

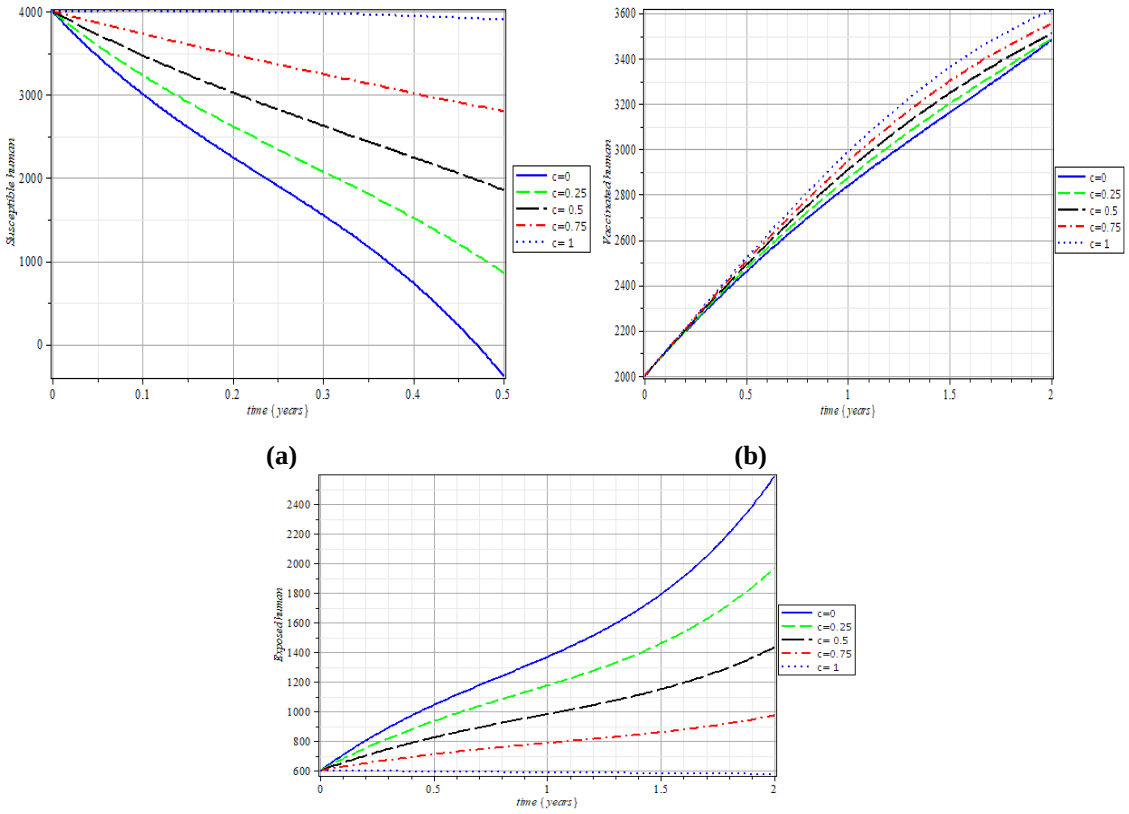

(a) **(b)**

(c)

Figure 3: Simulated population dynamics under public awareness intervention

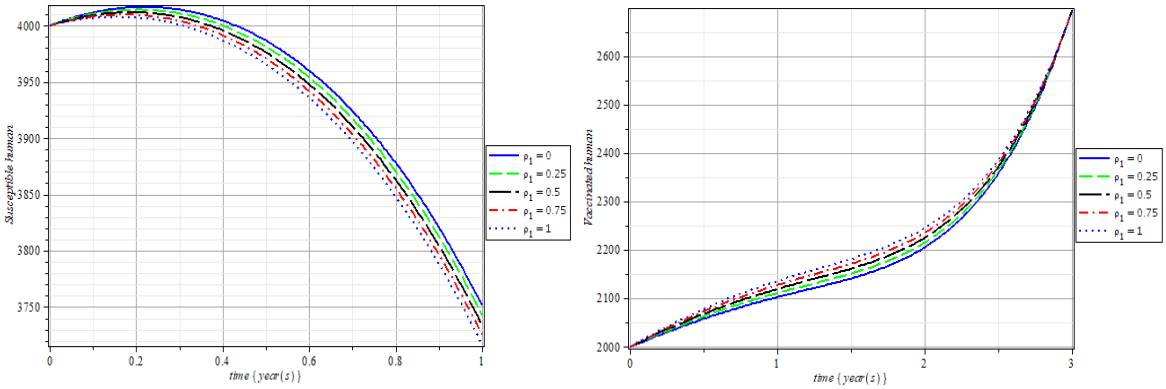

(a) (b)

Figure 4: Simulated population dynamics under childhood vaccination

Table 5: Numerical results of convergence test.

Variables	**Numerical relations**	**Results**
$S(t)$	$\xi_{s,6} = \frac{\|S_{n+1}\|}{\|S_n\|} = \frac{0.587894004 \cdot 10^{-5}}{0.1794208089}$	0.00003276621076<1
$V(t)$	$\xi_{v,5} = \frac{\|V_{n+1}\|}{\|V_n\|} = \frac{0.0000388231890}{1.014279416}$	0.00003827662120<1
$E(t)$	$\xi_{E,5} = \frac{\|E_{n+1}\|}{\|E_n\|} = \frac{0.000254777178}{6.668313583}$	0.00003820713812<1

$I(t)$	$\xi_{I,4} = \frac{\|I_{n+1}\|}{\|I_n\|} = \frac{0.00000913352148}{0.1988171047}$	0.00004593931440<1
$T(t)$	$\xi_{T,3} = \frac{\|T_{n+1}\|}{\|T_n\|} = \frac{0.0000734404281}{5.468124025}$	0.00001343064418<1
$R(t)$	$\xi_{R,2} = \frac{\|R_{n+1}\|}{\|R_n\|} = \frac{0.02688921733}{0.06781400000}$	0.3965142497<1

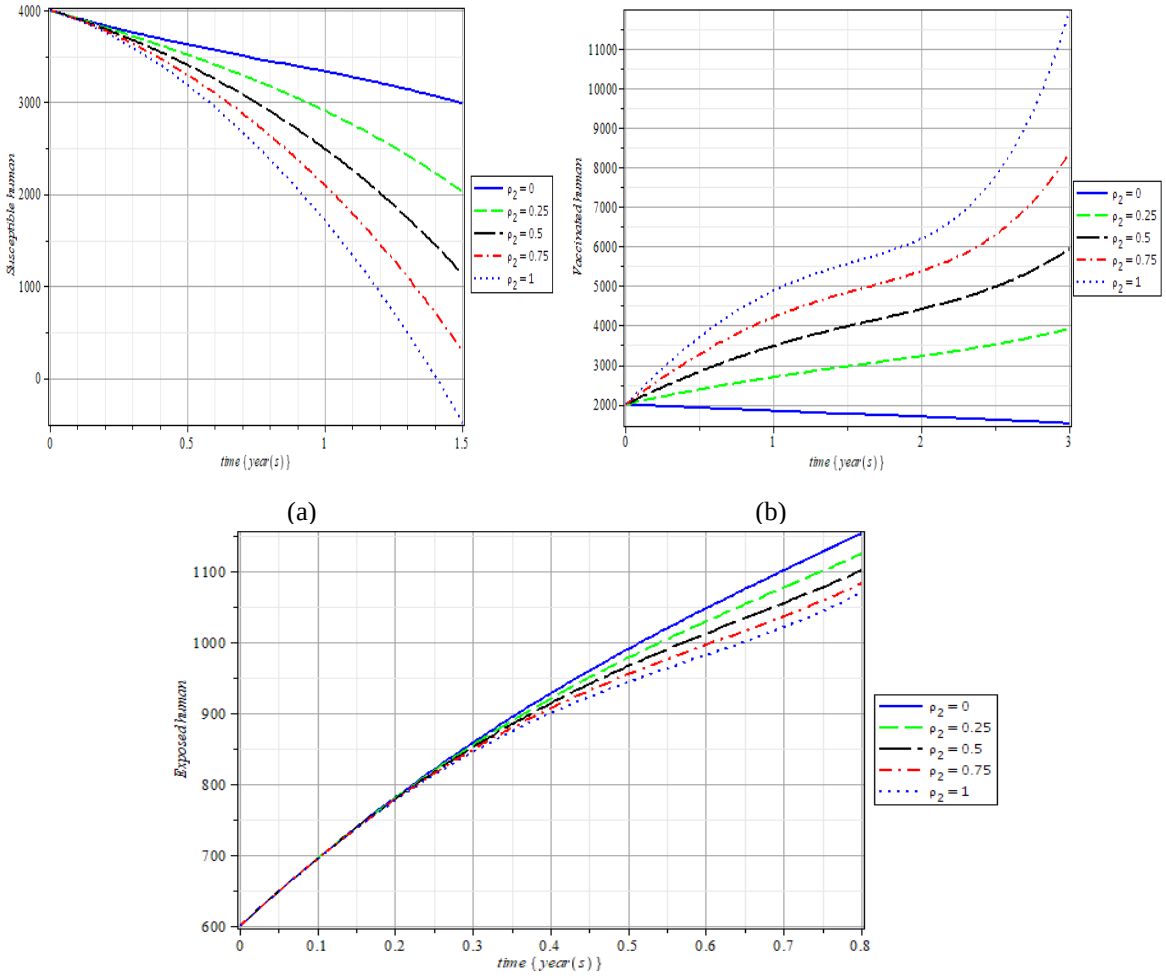

(a) (b)

(c)

Figure 5: Simulated population dynamics under adult vaccination

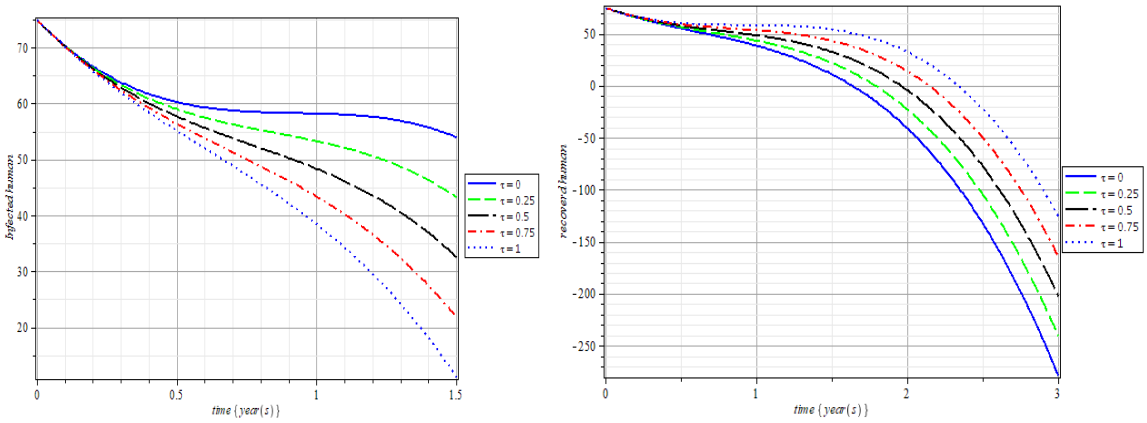

(a) (b)

Figure 6: Impact of treatment efficiency on infectious and recovered compartments

4. CONCLUSION

In conclusion, the study emphasizes the need for a comprehensive approach to tuberculosis control. The model identifies the combined-intervention threshold and sensitivity structure as the main analytical contribution. The LADM-based results suggest that coordinated awareness, vaccination, and treatment can reduce the effective reproduction number more strongly than isolated measures. The present study is not a comparative efficiency assessment of LADM versus RK4; a direct comparison with RK4 and other numerical schemes is recommended for future work. As recommendation, based on the model results, sustained awareness programmes, accessible vaccination strategies, and effective treatment coverage should be implemented together to reduce transmission and relapse risk. Health practitioners should collaborate with local communities to develop context-specific preventive measures.

Financial Support
No financial support was obtained for this research.

Acknowledgement
The author acknowledges the support of the academic staff of the Department of Mathematical Sciences, Osun State University, Osogbo.

Declaration
The author declares no conflict of interest.

REFERENCES

[1] World Health Organization, "Tuberculosis," Fact sheet, Mar. 24, 2026. [Online]. Available: https://www.who.int/news-room/fact-sheets/detail/tuberculosis

[2] C. Castillo-Chavez and B. Song, "Dynamical models of tuberculosis and their applications," Mathematical Biosciences and Engineering, vol. 1, no. 2, pp. 361-404, 2004, doi: 10.3934/mbe.2004.1.361.

[3] J. P. Aparicio and C. Castillo-Chavez, "Mathematical modelling of tuberculosis epidemics," Mathematical Biosciences and Engineering, vol. 6, no. 2, pp. 209-237, 2009, doi: 10.3934/mbe.2009.6.209.

[4] Z. Feng, C. Castillo-Chavez, and A. F. Capurro, "A model for tuberculosis with exogenous reinfection," Theoretical Population Biology, vol. 57, no. 3, pp. 235-247, 2000, doi: 10.1006/tpbi.2000.1451.

[5] I. Ullah, S. Ahmad, Q. Al-Mdallal, Z. A. Khan, H. Khan, and A. Khan, "Stability analysis of a dynamical model of tuberculosis with incomplete treatment," Advances in Difference Equations, vol. 2020, art. no. 499, 2020, doi: 10.1186/s13662-020-02950-0.

[6] Z.-K. Guo, H. Xiang, and H.-F. Huo, "Analysis of an age-structured tuberculosis model with treatment and relapse," Journal of Mathematical Biology, vol. 82, no. 5, art. no. 45, 2021, doi: 10.1007/s00285-021-01595-1.

[7] K. D. Dale, M. Karmakar, K. J. Snow, D. Menzies, J. M. Trauer, and J. T. Denholm, "Quantifying the rates of late reactivation tuberculosis: a systematic review," The Lancet Infectious Diseases, vol. 21, no. 10, pp. e303-e317, 2021, doi: 10.1016/S1473-3099(20)30728-3.

[8] G. Simorangkir, D. Aldila, A. Rizka, H. Tasman, and E. S. Nugraha, "Mathematical model of tuberculosis considering observed treatment and vaccination interventions," Journal of Interdisciplinary Mathematics, vol. 24, no. 6, pp. 1717-1737, 2021, doi: 10.1080/09720502.2021.1958515.

[9] T. L. Kang, H.-F. Huo, and H. Xiang, "Dynamics and optimal control of tuberculosis model with the combined effects of vaccination, treatment and contaminated environments," Mathematical Biosciences and Engineering, vol. 21, no. 4, pp. 5308-5334, 2024, doi: 10.3934/mbe.2024234.

[10] N. A. Menzies et al., "Progression from latent infection to active disease in dynamic tuberculosis transmission models: a systematic review of the validity of modelling assumptions," The Lancet Infectious Diseases, vol. 18, no. 8, pp. e228-e238, 2018, doi: 10.1016/S1473-3099(18)30134-8.

[11] G. Adomian, Solving Frontier Problems of Physics: The Decomposition Method. Dordrecht, The Netherlands: Kluwer Academic Publishers, 1994.

[12] A. M. Wazwaz, "The combined Laplace transform-Adomian decomposition method for handling nonlinear Volterra integro-differential equations," Applied Mathematics and Computation, vol. 216, no. 4, pp. 1304-1309, 2010, doi: 10.1016/j.amc.2010.02.023.

[13] P. van den Driessche and J. Watmough, "Reproduction numbers and sub-threshold endemic equilibria for compartmental models of disease transmission," Mathematical Biosciences, vol. 180, no. 1-2, pp. 29-48, 2002, doi: 10.1016/S0025-5564(02)00108-6.

[14] S. Marino, I. B. Hogue, C. J. Ray, and D. E. Kirschner, "A methodology for performing global uncertainty and sensitivity analysis in systems biology," Journal of Theoretical Biology, vol. 254, no. 1, pp. 178-196, 2008, doi: 10.1016/j.jtbi.2008.04.011.

[15] World Bank, "Birth rate, crude (per 1,000 people) - Nigeria," World Development Indicators, 2023. [Online]. Available: https://data.worldbank.org/indicator/SP.DYN.CBRT.IN?locations=NG

[16] Institute for Disease Modeling, "SEIR and SEIRS models," EMOD Tuberculosis Model Documentation, 2024. [Online]. Available: https://docs.idmod.org/projects/emod-tuberculosis/

[17] G. A. Colditz et al., "Efficacy of BCG vaccine in the prevention of tuberculosis: meta-analysis of the published literature," JAMA, vol. 271, no. 9, pp. 698-702, 1994, doi: 10.1001/jama.1994.03510330076038.

[18] R. S. Wallis, "Mathematical models of tuberculosis reactivation and relapse," Frontiers in Microbiology, vol. 7, art. no. 669, 2016, doi: 10.3389/fmicb.2016.00669.

[19] K. Abbaoui and Y. Cherruault, "Convergence of Adomian's method applied to differential equations," Computers & Mathematics with Applications, vol. 28, no. 5, pp. 103-109, 1994, doi: 10.1016/0898-1221(94)00144-8.